BillikenSat-II: The First Bio-Fuel Cell Test Platform for Space

Sanjay Jayaram
Assistant Professor
Aerospace and Mechanical Engineering, Saint Louis University, Saint Louis, Missouri; 314-977-8212;
sjayaram@slu.edu

Darren Pais, Sonia Hernandez, Paul Lemon, Nathaniel Clark, Benjamin Corrado, Brian Vitale, Justin Kerber, Elena Nogales, Jorge Moya, Robert Arechaderra*
Undergraduate Students, * Graduate Student
Space Systems Research Laboratory, Parks College of Engineering, Aviation and Technology, Saint Louis University, Saint Louis, Missouri; 314-977-8440
cubesat@slu.edu

ABSTRACT

Saint Louis University's Space Systems Research Laboratory has designed and built an earth orbiting student project called BillikenSat-II that will carry a payload to test a Bio-Fuel Cell experiment. This satellite conforms to the CubeSat standard and is a pico-class satellite weighing a maximum of 1 kg and having dimensions of 10 cm x 10 cm x 10 cm. The satellite is to be launched on a converted Russian ICBM via the DNEPR program, in coordination with California Polytechnic and State University (CalPoly, San Luis Obispo, CA) at a launch date to be determined. This paper will describe BillikenSat II's scientific objectives and the Bio-Fuel Cell test platform design to carry out the scientific objective as well as student designed and built BillikenSat-II spacecraft bus, its various subsystems and project management.

Mission Statement: To design, build, test and launch a pico-satellite that fits the CubeSat standard and incorporates a Bio-Fuel Cell test experiment as payload.

INTRODUCTION

The CubeSat concept is a program conceived by Professor Robert Twiggs of Stanford University's Space Systems Development Laboratory to expose students to all aspects of satellite design, manufacture and operation.[1,2] Ideally intended for university programs, CubeSats are planned to go from design through construction and testing of a finished product within approximately a one-year timeline. The design constraints of the CubeSat concept limit the total satellite mass to 1 kg and within a 10 cm cube.

The design process of BillikenSat-II as represented in this paper focuses on ensuring that the satellite serves as an effective platform for the Bio-Fuel cell experiment, while ensuring that the CubeSat constraints are met at every step. The trade-offs between designing an effective experiment and meeting the requirements of the launch program are emphasized in this paper, and constitute the primary reason behind our decision to design a satellite system that is simple in structure and operation, and yet effective to carry out the experiment.

BillikenSat-II is being built by the Space Systems Research Laboratory (SSRL) at Saint Louis University in Saint Louis. BillikenSat-II will be the second satellite built by Saint Louis University. The project is entirely student run, with faculty members acting as advisers. First and foremost, BillikenSat series is an educational project. Students are involved with every part of the satellite, including but not limited to: designing the satellite, designing and constructing onboard experiment and all subsystems, commissioning a ground station to

control and communicate with the satellite, testing the engineering and flight models, and contributing to public outreach and web site development.

BillikenSat-II is designed and fabricated on a low-cost budget of less than $50,000, including launch, by using mostly off the-shelf hardware and software. The first section of the paper describes the payload experiment and design including the challenges in designing a pressure chamber. The second section describes various subsystems and the project management aspects.

SCIENCE MISSION

Science Context

The Bio-Fuel cell experiment onboard BillikenSat-II is designed in collaboration with the Minteer Research Group at the Department of Chemistry, Saint Louis University. The reasons for incorporating the Bio-Fuel cell as payload on BillikenSat-II are manifold. Firstly, Bio-Fuel cells constitute a cutting edge area of research that is receiving increasing attention in the scientific community. Secondly, the Minteer Group has advanced technologies and patented research in this area, thereby providing the BillikenSat-II group a unique opportunity for extensive collaboration and interdisciplinary work. Finally, the versatile nature of Bio-Fuel cells renders them especially suited for the stringent requirements of long-term space missions (vis-à-vis Moon, Mars and Beyond) and thereby provides opportunities for future use and commercial development of this technology. BillikenSat-II is designed to be a first-step 'proof of concept' vehicle, illustrating the viability of Bio-Fuel cells in the harsh space environment.

PAYLOAD

Bio-Fuel Cell

The Bio-Fuel cells consist of two plates, a cathode and an anode. The anode will hold the fuel reservoir while the cathode will be an air permeable plate. The two sides of the fuel cell are separated by a membrane made of Nafion[3], which contains the enzymes necessary for the chemical reaction. When the fuel, enzymes and air react, they produce water and electricity as by-products. Bio-Fuel cells have been tested on Earth but their operation in space has never been studied. Running fuel cells in a harsh LEO environment presents many challenges, among them radiation, large temperature changes between sunlight and eclipse, and a vacuum environment. In order to surmount these challenges, a unique approach has been designed. Normally, the Bio-Fuel cell requires two large metal plates on either side of the cell to provide necessary pressure to ensure an adequate connection between the cell components. These plates are large and relatively heavy for a Pico-satellite configuration. Thus, instead of using separate plates to supply pressure, the two fuel cell plates are machined out of Stainless Steel 416. The steel will be gold plated in order to prevent corrosion and increase conductivity. The Nafion membrane is placed between the two plates and the assembly will be bolted together to ensure proper contact. In order to prevent a short circuit from one plate to the other through the bolts, Phenolic bushings and washers are used to prevent any metal-to-metal contact. The final design of the bio fuel cell is shown in Fig. 1. The stainless steel also resists corrosion due to the Bio-Fuel which is stored in the anode bipolar plate.

Figure 1: Finished Gold Plated Bio-Fuel Cell

Payload Tank

The fuel cell must be in an oxygen rich environment in order to function; therefore, a pressure tank was designed to contain the fuel cell in a 50-psi environment. The pressure tank will consist of two components fabricated using PEEK (PolyEtherEtherKetones) material. PEEK is a

thermoplastic with very favorable characteristics for space applications (low thermal conductivity, high tensile strength, good out-gassing properties). Heat conducted from the structure to the payload tank was a concern due to the stringent operational range of the fuel cell. PEEK is specially suited in this case as its thermal conductivity is 1/1000th that of aluminum. A high tensile strength is also desired for the payload tank since it is a pressure vessel operating in a vacuum environment. Again, PEEK provides the necessary high strength characteristics (tensile yield stress of 14000 psi[4]). The first tank component is a square plate 80 mm on a side and 2.5 mm thick. The second component is a cylindrical tank section with a 30 mm radius, a depth of 21.5 mm and a thickness of 3 mm set into a plate matching up to the first component. The minimum tank thickness was calculated using the cylindrical pressure vessel circumferential stress equation[5]. This thickness was calculated to be only a fraction of a millimeter, but in order to allow for ease of handling, manufacturing and margin of safety, a thickness of 3 mm was chosen. An elastomer seal will be sandwiched in between the two PEEK components in order to ensure a proper air-tight seal. The design is shown in Fig. 2.
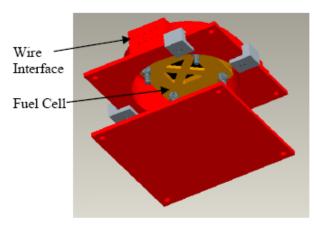

Figure 2: Payload Tank Design: Exploded View

The tank must undergo pressurization and testing on the ground, necessitating a means to add oxygen to the already sealed tank. A block of material was added to the cylindrical portion of the tank design with several concentric holes of different diameter and varying depths, drilled into the extra material. A PEEK pipe with an outer diameter of 1.6 mm and an inner diameter of 0.127 mm will be fed all the way into the inner portion of the tank. A ferrule will then be placed around the pipe, and finally a screw will be slid along the pipe up to the ferrule as can be seen in the exploded view in Fig. 3. This mechanism clamps down and seals a thin pipe into the tank, through which oxygen can be fed to pressurize the tank, and is widely used for similar applications.
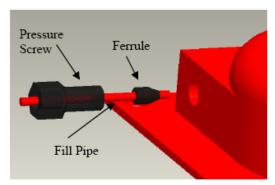

Figure 3: Pressure Interface

The payload must also be able to communicate with the rest of the satellite in order to conduct the necessary mission experiments and provide data. Several different electrical components must be incorporated within the payload tank to allow for proper monitoring and control of the fuel cell. The electrical components include the wires to the fuel cell itself, a pressure sensor, the Thermofoil® heater, and a temperature sensor. No computations will be conducted within the payload because the pressurized volume inside the tank must be kept to a minimum to reduce structural weight and complexity. A simple approach is undertaken in order to pass the necessary wires into and out of the payload tank. Solid core wires will be stripped of their insulation, coated in epoxy, and run through the corresponding holes in the payload tank. The holes will also be filled with slow curing epoxy and the entire assembly will be allowed to set for the time specified by the epoxy. The method for securing wires into the payload tank was pressure tested at two temperature extremes, and the method worked flawlessly at each extreme. Once complete, the payload tank will be able to withstand up to 1500 psi without failing structurally. It will also provide the fuel cell with enough oxygen to operate for up to 10 hours, while gathering vital information on the

temperature and pressure of the environment within the tank, along with fuel cell experimental data. The wealth of data collected by this experiment will provide information regarding the feasibility of Bio-Fuel cell applications in space.

Payload Monitoring

The monitoring system for the Bio-Fuel cell consists of a potentiostat and thermal sensors. A potentiostat is a measuring and control device that keeps the potential of working electrode at a constant voltage with respect to a reference electrode. The potentiostat was made with a digital to analog converter in conjunction with an op-amp that drives the working electrode to a voltage level defined by the microprocessor. A current to voltage amplifier is then used to find the current through the Bio-Fuel cell. This voltage is then sampled by the analog to digital converter built into the microprocessor and logged to memory. To ensure that the fuel cell is not drained by internal resistances of the potentiostat prior to the experiment, the cell is isolated using reed relays that are turned on at the beginning of each experiment and off upon completion.
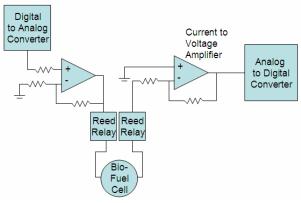

Figure 4: Potentiostat for measuring the fuel cell

Testing Methodology

To determine the Bio-Fuel cell potential the cell is driven at 1.2 V and stepped down to 0 V throughout the course of the experiment in 1 mV intervals. This happens over a 400 second interval. The initial starting bias of 1.2 V is chosen as it is the maximum cell potential expected. The current is then determined using a simple ohms law calculation from the current to voltage amplifier. Samples are taken every 0.0125 seconds, then averaged and logged for each mV step taken.
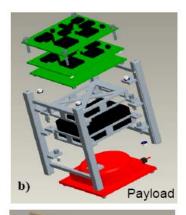
STRUCTURE

Satellite Bus Design

The main satellite structure consists of two side panels and a battery box. Each side panel has crossbars joining two rails together as one piece, to be machined out of aluminum 6061-T6. Aluminum 6061 is an ideal material for the structure due to its affordability, similarity to Aluminum 7075 in thermal expansion, and relative ease of machining. The two panels will be joined together by the battery box, which will consist of two identical components bolted together to house all four batteries, while also providing the backbone of the structure (Fig. 4a).

The side support panels serve multiple purposes for the mission. First, they integrate the side rails into the satellite to ensure that the satellite is deployed properly once in orbit. Second, they provide a means to support all the internal components necessary for mission success, and finally, they hold the exterior panels with the solar cells in place. Several designs were considered, with the goals of reducing complexity and weight (by using a minimum number of fasteners), resisting excessive deformation on launch due to vibrations and g- loading, and allowing proper placement of necessary mission sub-systems. The surfaces of the rails must be anodized to prevent cold welding to the P-POD in orbit and any unwanted electrical conductance. The rails also must incorporate small holes at the top and bottom to allow for deployment springs and a kill switch. The kill switch prevents the satellite from activating while still in the P-POD. The side panel utilizes two 4 mm square cross sections, 83 mm in length support cross-bars running from one rail to the other. These crossbars are placed at the top and bottom, while still allowing spacing as per CubeSat requirements, and room for exterior solar panels. The support panels also use slots running the height of each rail on one interior side to allow for exterior solar panels to slide into place for easy installation as well as access to internal

components. Two of the exterior panels will be installed in such a fashion, with the remaining four screwed in place directly into the support crossbeams.

The battery box has enough interior space for four batteries, wiring, and insulation. The design was optimized for a minimum mass while preserving the interior space needed as well as providing adequate support for the two side panels. Mass was saved by removing material wherever possible without compromising the structural integrity. The exterior panels will be manufactured from Printed Circuit Board material to allow for mounting solar cells, as well as providing strength and stiffness to the aluminum support panel, once installed. These exterior panels (Fig. 5b) will be installed using small screws and epoxy. The panels will be painted white on the space facing side to reflect as much thermal radiation as possible and keep the satellite temperatures in a more favorable range for the electronics.
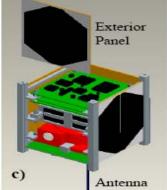

Figure 5b, 5c: Satellite Bus Exploded View and Assembled View showing side panel and antenna

A reliable antenna design was also needed to allow for proper communications once the satellite is placed in LEO. The Nitinol shape memory alloy wire was chosen for the antenna material because it can operate as an antenna while also serving as part of the deployment mechanism. The alloy tends towards a specific shape, in this case a straight line. When that shape is altered by a constraining mechanism, the wire will return to the original shape as soon as the constraining element is removed. Nylon wire was chosen to constrain the antenna, intertwined with Nichrome wire that will melt the nylon when a current is passed through it. Once the nylon is melted, the Nitinol will be free to spring back to its straight configuration and begin communications. The antenna itself is attached to the exterior panel of the top and bottom of the satellite using silver epoxy, which provides both a structural and electrical connection.

Finite Element analysis was done to ensure that the designed structure withstands launch load conditions. The results provided with the satisfactory numbers with maximum displacement of the mount found to be 0.000148 millimeters at the interior most corner for the worst case scenario and the maximum stress was 0.3 MPa, which is well under aluminum 6061's ultimate stress or yield stress.

Manufacturing

The entire satellite structure was manufactured based on the DFMA (Design for Manufacturing and Assembly) principle. Hence, a large amount of time was devoted to the fabrication of the structural components, including the aluminum side panels, battery box, payload tank bottom plate, payload tank clips, payload tank wire interface, and the main payload tank.

The major challenges involved with the manufacturing involved the high degree of precision demanded by the standard, with outer dimensions satisfying a tolerance of plus or minus 0.1 mm. The relatively small size of the bus also created a few difficulties, as the equipment needed for such minute cuts was not able to reach as far as more common, larger equipment. Several of the openings cut into the battery box to save mass and

allow for wires to be drawn out had to be repositioned slightly due to interference between the mounts and the mill bit. Once the design was modified to move the openings further from the mounts, the fabrication was able to continue to completion. Manufacturing of many critical components, including the side panels, battery box, bipolar fuel cell plates, and payload pressure clips is already completed. A picture showing the completed satellite bus structure is presented in Fig. 6.
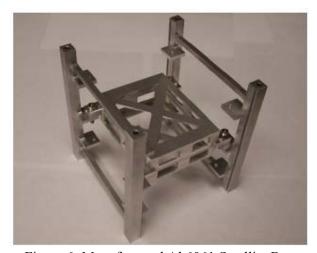

Figure 6: Manufactured Al 6061 Satellite Bus

The antenna deployment and attachment methods have been successfully tested. The silver epoxy was used to attach the antenna to the structure and also to achieve needed electrical conductivity. The epoxy was set at 150ºF while the antenna was constrained in a coiled form by the nylon. The Nitinol wire used does not alter its base shape unless heated to several hundred degrees Fahrenheit, therefore the 150ºF curing did not affect the shape of the antenna after deployment. The Nitinol wire was deployed once the epoxy had set, and antenna immediately deployed into the desired form once the nylon snapped. A picture a successful antenna deployment test is presented in Fig. 7.

The total satellite mass has been calculated to be approximately 906 grams allowing 94 grams for contingency purposes. Additions such as wiring and epoxy are difficult to accurately estimate, but their total mass is expected to fall well within the contingency buffer.
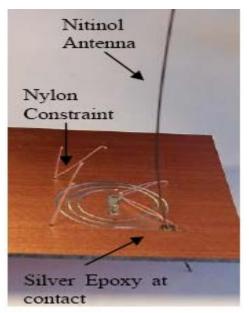

Figure 7: Antenna Deployment

THERMAL ANALYSIS AND CONTROL

BillikenSat-II will be operating in Low Earth Orbit, at around 700 km altitude (based on DNEPR launch provider's data). In this environment, both infrared radiation and albedo (reflected solar energy) must be taken into consideration, along with the direct solar radiation. These forms of radiation are the only sources of heat for the satellite since it is operating in the vacuum of space. Heat is transferred via convection, conduction, or radiation. Radiation is the main mode of heat transfer in space because it requires no medium and is actually more efficient in a vacuum. Because there is no air either in space or the main structure of the satellite, convection plays no part in the thermal environment. Conduction is important when analyzing the heat transfer from the main structure to the internal components.

Radiation heat transfer is greatly dependent upon the surface properties of the body as the radiation incident on a body is absorbed within the first few microns. The first important material value is the absorptivity α. Absorptivity is the ratio of absorbed radiation to the incident radiation. The emissivity ε is the ratio of radiation emitted to the radiation emitted by a blackbody (an ideal body that absorbs and emits all incident radiation). The

ratio of these two values is a good predictor of behavior for a material exposed to thermal radiation. For example, polished aluminum has a ε/α ratio of 3.0 which indicates that it is more effective at absorbing radiation than emitting it, making it warmer, when exposed to the same environment, than anodized aluminum, which has a ε/α ratio of 0.17.

To find the true temperature limits of the satellite's environment, it is necessary to find the temperature equilibrium environment. This is done by finding the radiation absorbed and the radiation emitted, setting these two values equal to each other, and finding the resulting temperature. The resulting temperature will be the absolute highest or lowest possible temperature. This calculation is shown here for the maximum temperature situation of two sides equally exposed to direct sunlight and one face exposed to direct albedo and Earth infrared normal to the face and minimum temperature situation of eclipse (only Earth infrared normal to one face).

Dynamic Modeling

The dynamic thermal modeling and analysis was done using computer simulation to verify the analytical solutions. CUBESIM software was used for this purpose. Specifically, seven degrees of freedom thermal model was used for accuracy purposes. The result obtained through CUBESIM is shown in Figure 8.
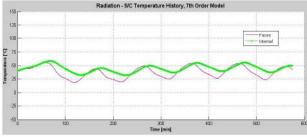

Figure 8: Seven Degrees of Freedom CUBESIM simulated temperatures

The temperature range given in this CUBESIM model is fairly high when compared to the expected range for this satellite, and is also high compared to the analysis done for other CubeSat satellites. This could be due to any number of things, the most likely of which is the geometric differences between CUBESIM assumptions and

BillikenSat-II. This model does give a satellite temperature that is survivable by all components with the exception of the batteries and payload, which are discussed in detail later in this paper, but it does not seem right for a structure in space, with limited heat generation, to stay above room temperature $(25^{\circ}C)$ at all times. Because of the intuitive sense that BillikenSat-II should experience a greater temperature range in orbit, it was decided that a hand calculation was necessary to find the solution for this specific satellite structure. Following equations were used to further perform the thermal analysis calculations.

$$Q_{total} = G\,\alpha_{avg}A_i - \varepsilon_{avg}\sigma A_{total}T_0^{\ 4} \qquad (1)$$

Equation 1 gives the energy transfer rate is highly dependent on the temperature of the body. This is continuously changing as the satellite is exposed to the orbital environment, so the satellite temperature must be found. However, this is directly related to the energy transfer rate as shown in Eq. (2) where C_{P_i} is the specific heat component i, m_i is the mass of component i, and T_f is the temperature of the satellite after time t. Since the energy and temperature are related as they are, an iterative process of going from Eq. (1) to Eq. (2) back to Eq. (1) and so on must be used to find the maximum and minimum temperatures experienced by the satellite.

$$Q_{total}t = c_{p_i}m_i(T_f - T_0) \qquad (2)$$

For this analysis the two main sides, the six side panels, the permanent magnets, the battery box, the electrical boards, and nuts, bolts, and washers were considered to be the heat-conducting structure. After approximately 10 hours, it was found that the upper and lower temperatures experienced each orbit converged to the temperatures:

$$T_{max} = 314.4K = 41.2^0C$$
$$T_{min} = 223.1K = -50.1^0C$$

This is not to say that the satellite reached equilibrium, but that there is an upper temperature of 314.4 K that is reached in sunlight and a lower temperature of 223.1 K that is reached in eclipse

and that BillikenSat-II reaches these temperatures each time it orbits the earth. This analysis is good as a second approximation because it gives a temperature range tighter than just the equilibrium temperatures. It is still lacking as a true representation of temperature over time because it only calculates the temperature twice an orbit, once at the end of sunlight and once at the end of eclipse. To accurately represent the temperatures experienced over time, the time t from Eq. (2) needs to be a small change in time. A MATLAB® program was written to calculate and plot the temperature with a time interval of one second, with the resulting graph in Fig. 8. This is the final refinement in the structural temperature analysis, and it results in an operating range of -20°C to 35°C. It takes into account all known factors, including internal heat generation from the electronics.
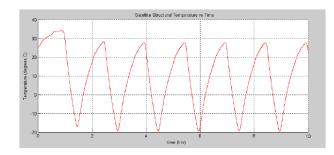

Figure 9: Plot of temperature over time for the BillikenSat-II structure

Payload Active Thermal Control

The payload of BillikenSat-II is the most thermally sensitive component. The experiment must remain between 4°C and 40°C at all times. In order to protect the payload, an active controlled resistance heater is used. High-end temperatures can be adequately addressed by the payload box, which is made from PEEK polymer, a material with low thermal conductivity (0.25 W/mK). To prevent the payload from freezing, a heating system is used. The heater is an 8 Ohm Kapton Thermofoil™ Heater from Minco© (Fig. 10) which produces 1.13 Watts of heat when running at 3.3 volt source provided by the power system. A platinum Resistance Temperature Detector from US Sensors, part PPG101C1, is used to detect temperature inside the payload. The single platinum element RTD allows for a smaller part with greater sensitivity and is just 1.24 mm x 1.7 mm x 2.41 mm in size.
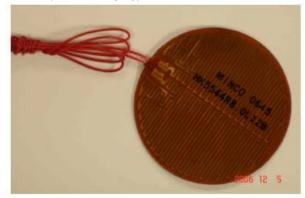

Figure 10: Kapton Thermofoil Heater

Figure 11 shows the feedback loop for regulating the temperature inside the payload. It was calculated that the heater should be on for just 14 minutes every 18 hours to regulate the temperature.
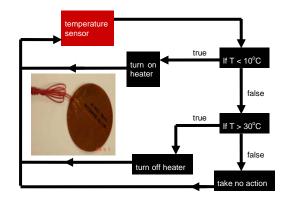

Figure 11: Feedback Control for Temperature Regulation

ATTITUDE CONTROL SYSTEM

Since the mission of the BillikenSat-II is to test a BioFuel Cell experiment in space and communicate the test results to earth, the satellite doesn't require stringent pointing requirements. The only pointing requirement is for the antenna to communicate with the ground station. So, BillikenSat-II has nominal attitude constraints – The satellite needs to be stable (no high frequency/high amplitude oscillations) and the attitude must enable effective ground communication (antenna parallel to Earth's

surface in the communication window). After trade-off analysis, a passive magnetic attitude control system, with hysteresis dampers, will be used for attitude control (illustrated in Fig. 12). The choice of a completely passive system was driven by two key constraints – 1) the satellite control system must be simple and free from failure, and 2) the control system must be inexpensive in terms of cost, mass and computational power requirements. For failure proof communication with the satellite, the only requirement is to deploy the antenna parallel to the earth's magnetic field (shown in figure below).
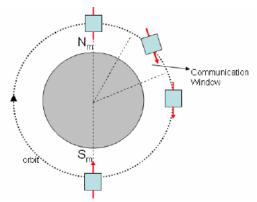

Figure 12: Earth's Magnetic Field and Communication windows

Based on the mission requirements of BillikenSat-II, it is not required to determine the attitude of the satellite in orbit. Since it will be beneficial to measure the rotation rate of roll (velocity) axis of the satellite, one gyroscope is used to measure the rotation rate of the spacecraft. As a secondary technical mission, BillikenSat-II will have two more gyroscopes in the yaw and the pitch axis to measure those rotations as the satellite moves from poles to poles in the orbit. The next section shows the orbital analysis.

Orbital Simulation

BillikenSat-II orbital analysis is performed using STK for a 24-hour period, and is represented in Fig. 13. In the 2-D graph shown, the white traces represent when the satellite is going to be in sunlight, and the dark blue traces represent when it will be in eclipse. Study of sunlight and eclipse times indicate that the satellite will be in sunlight about double the time that it will be in eclipse. More specifically, for one revolution around the

Earth, the satellite is in sunlight for 62 minutes, after which it is in eclipse for 37 minutes. This process repeats itself with slightly varying sunlight and eclipse times for each orbit. The exact position and the orbital elements of BillikenSat-II after launch deployment will be obtained and provided by NORAD as a Two Line Element.
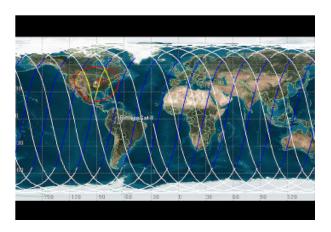

Figure 13: STK Orbital Analysis

Magnetic and Hysteresis Torques Modeling

In order to accurately size the permanent magnets (to pick dipole strength) and design the control system, the dynamic attitude of the satellite is modeled, taking into account the magnetic torques acting on the satellite. To this end, a quaternions-based dynamic model of satellite attitude that incorporates permanent magnet alignment and non-linear hysteresis damping effects is designed.

To model and simulate the Earth's Magnetic Field, the IGRF mathematical models are used. The IGRF expresses the scalar magnetic potential as a series expansion function of distance from the Earth's center, latitude and longitude. The approximate L-Shell model of the magnetic field also provides a good qualitative description of the magnetic field lines. At a given magnetic latitude λ, for a given L-value (measured in Earth Radii, corresponding to a given field line), the field radius, which is the distance in Earth Radii from an idealized magnetic dipole at the Earth's center can be calculated.

Hysteresis magnetic materials are much like permanent magnets in their function, except that they are of significantly higher permeability. This means that under the influence of a changing weak external magnetic field (like the Earth's field), the hysteresis materials tend to exhibit realignment of dipoles and change in magnetic domain boundaries. These changes result in frictional dissipation of energy at the molecular level, a phenomenon known as hysteresis dissipation. In order to maintain system equilibrium on permanent magnet and field alignment, the hysteresis materials must have their dipole axes orthogonal to the permanent magnets. Hysteresis materials are defined by three key parameters- the saturation induction (Tesla), the remanent induction (Tesla) and the coercivity (Ampere/meter). Using these parameters, the hysteresis loop outer boundaries can be approximated as tangent functions (Eq. (3)) and depicted in Figure 14.
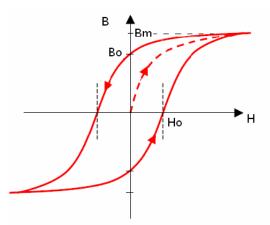Equation 3 here

Figure 14: Variation of magnetic induction (B) with external magnetizing field (H) for a hysteresis material.

Attitude Simulation

With the known Moment of Inertia for the BillikenSat-II, two scenarios were simulated, one without hysterisis damping and one with hysterisis damping. Scenario 1 of the set of simulations is for all initial conditions (angular velocities and Euler angles) set to zero, for a satellite having only permanent magnets for stabilization and no hysteresis dampers.The results of this simulation

are presented in Fig. 15 for one full orbit at different permanent magnet strengths. Notice that the higher permanent magnet strength implies a higher frequency of oscillation and higher oscillation amplitude as expected. Also, notice that the satellite does pitch through the necessary 360in one orbit, illustrating that it oscillates about the geo-magnetic field with maximum amplitude of about 20 degrees.
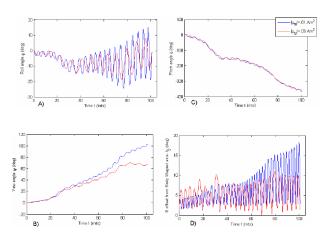

Figure 15: Scenario 1-Permanent magnet response a) Roll angle response b) Yaw angle response c) Pitch angle response d) B-offset: magnet deviation from field lines, notice higher amplitudes and oscillation frequencies for higher magnetic dipole moment (curves in red). Dipoles: Blue 0.03 Am^2, Red: 0.01 Am^2.

In Scenario 2, the effects of adding hysteresis damping to mitigate the high-amplitude oscillations observed for the higher permanent magnetic dipole stabilization in Scenario 1 (Fig. 15) are simulated. Notice the smoothening of the pitch and yaw curves, as well as the reduction in field offset, because of the mitigation of oscillations by the hysteresis material. The hysteresis material have a lesser long-term effect on mitigating roll oscillations as they do not exert moments along the roll axis following field alignment (because they are perpendicular to the alignment axis of the permanent magnets). However, roll oscillation amplitudes are significantly mitigated as seen in Fig. 16.
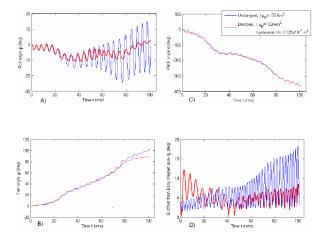
Figure 17: Scenario 2-Permanent magnet with hysteresis response a) Roll angle response b) Yaw angle response c) Pitch angle response d) B-offset, notice yaw and pitch damping, roll amplitude

ELECTRICAL SYSTEMS

In order to support the mission of BillikenSat-II, an integrated electrical system was developed to monitor the health of the satellite, perform experiments on the Bio-Fuel cell, and communicate with the earth. In Fig. 17 a block diagram shows how the electrical systems interact with each other and the other satellite systems.
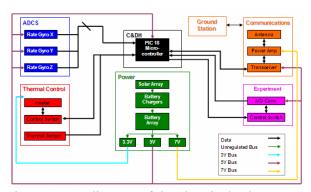

Figure 17 : A diagram of the electrical subsystems from a high level perspective.

All of the electronics are housed on three PCBs that are each 8cm by 8cm. There are boards for command & data handling and payload, power, and communications. All three boards have a common set of pins that transfer power and control signals that need to cross between various boards.

They mount to the common connectors on the rails of the CubeSat and are interchangeable in order.

COMMAND AND DATA HANDLING

The C&DH subsystem is responsible for accepting input from each of the subordinate subsystems, disseminating the data, and then outputting the correct response to the involved subsystem. On BillikenSat-II a PIC18F4523 microcontroller was chosen to perform this task. When selecting this microcontroller many factors influenced the decision. Most importantly the microcontroller must have low power consumption and sleep states that allow wake up from external devices, such as the radio. Ease of interfacing to external devices was also a major factor. The satellite will have SPI control to a DAC, thermometers, and microSD cards. The experiment also dictates a 12 bit ADC to achieve the resolution needed to properly compare to the results from the laboratory. Multiple I/O lines are required to control the multitude of FET based switches for heaters, antennas, and other control logic. An ANSI C compliant device was also required for code portability and ease of coding. Finally a large code base, competent user community and full documentation are available for the PIC18 series microcontrollers.

The PIC18 runs off of an external crystal oscillator of 4MHz for the main clock. Devices are attached to SPI port such as rate gyros and thermometers that monitor the condition of the satellite. The microcontroller is programmed via a 5 pin in circuit debugging header. The header also allows for a computer to be attached to the satellite and break points to be set for debugging the code while on actual hardware.

External Memory

The microcontroller interfaces to a microSD card for external storage through the SPI mode that is specified for in the MMC protocol. When storing data on the microSD card, the card is broken up into 3 sections where identical sets of data are stored. In addition, all data placed on the card is first hamming encoded in a 15 to 11 scheme, allowing errors to be fixed, or at least detected, if it is more than one bit upon retrieval. When data is retrieved from the card, all three locations are

looked at and compared against a hamming decoder. The first set that passes the hamming decode is then used by the system. If all packets are corrupt the retrieve is run again and the error is logged.

POWER

The Power subsystem is responsible for the generation, storage, and distribution of electrical power on board BillikenSat-II. There are two sources of power on board the satellite, solar panels and a Li-ION battery array. The satellite is launched with a full charge on batteries and all additional energy needed must be generated by the solar cells. The solar array is comprised of ten UTJ solar cells. These solar cells have a low mass, 3.085 grams per cell, and high efficiency, 25.1% efficient at beginning of life. They have a maximum power point current density of 14.9 mA/cm^2 and a maximum power point voltage of 2.45V. When exposed to sunlight at a normal angle of incidence, these cells will produce a current of approximately 550mA. The power developed from the solar array has two functions: first to power the charge management IC and second to contribute to the unregulated power bus during periods of low light or eclipse. Assuming that the voltage produced by the solar array is greater than the threshold level of the charger IC, the batteries will charged. However, when the satellite is in a region of low light or eclipse, the power is redirected to the unregulated bus by the charge cut-out from the charger IC. The battery charge management IC, a TI bq24004, is capable of providing a continuous charging current of 1.2A to the battery array. The charging circuit and battery packs have intelligent charging features that turn charging off at high and low temperatures, as well as preventing discharge and charging at maximum levels to keep the Li-ION cells from exploding.
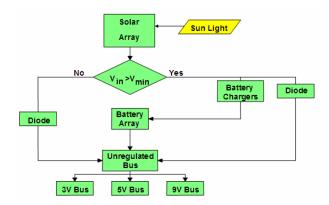

Figure 18: Power subsystem architecture

The storage of power onboard BillikenSat-II employs an array of four lithium-ion batteries in a parallel/series configuration. These batteries have a low mass, 41 grams per battery, and no memory effect. At full charge these batteries have a nominal voltage of 3.7V producing a bus voltage of 7.4V. The nominal operating capacity for these batteries is 1.8Ah at the discharge rate shown in Fig. 19.

Subsystem	Eclipse	Sunlight	% of the time active	Power consumed (mWh)
ADCS	Inactive	Active	6.25%	5.6
C&DH	Active, LP	Active, FP	25%	165
COMM	Stand-by	Stand-by	75%	112.8
		Transmit	12.5%	
		Receive	12.5%	
Thermal	Active	Inactive	1.3%	14.8
			Total:	298.2

Figure 19: Power consumption breakdown by power consumed and orbit location

DC/DC Converters

The distribution of electrical power is accomplished by using the unregulated voltage bus and stepping up or stepping down the voltage to the appropriate levels by way of DC/DC converters. There are three different regulated voltage busses on board BillikenSat-II: 3.3V, 5V, and 9V. These regulated voltage busses distribute voltage at the appropriate magnitude to the various auxiliary subsystems.
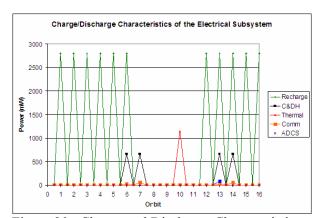
Figure 20: Charge and Discharge Characteristics of the Electrical Subsystem

The bus voltages were chosen based on a careful analysis of the requirements of each system. The C&DH and communications require 3.3V, the ADCS system requires 5 volts for the gyroscopes, and the power amplifier requires 9 volts. DC/DC converters are used to take the unregulated bus to the required busses.   Texas Instruments PT5100 converters were chosen due to their large input range and high current ratings.   Three separate devices were used for each rail.

Power States Near Launch

Prior to launch, the satellite will be have no power. The satellite includes a remove before flight pin as well as P-POD switch. The remove before flight pin is removed when the satellite is loaded into the P-POD. The P-POD switch is a small switch that is placed on the end of the satellite frame and is triggered when the satellite separates from the P-POD and the other two satellites with which it is launched.

COMMUNICATIONS

The communications subsystem allows the data gathered by the spacecraft to be received by ground stations and allows operators to send commands to the satellite.   This communications link is achieved using a 70cm half-duplex transceiver. The 70cm band was chosen based on the amateur radio allocations permitting the satellite to operate with without additional FCC licenses other than for the operators. A full duplex system using 70cm and 2m was considered but was not pursued due to the additional complexity

and long antenna lengths required. A number of modes were looked at including CW, AFSK, ASK, and PSK, however FSK was chosen due to its ability to work in a nonlinear system, making the amplifier more efficient and easier to build. FSK also is commonly found on many amateur radios allowing many ground stations to be able to talk with BillikenSat-II.

Transceiver Design

An IC transceiver solution was chosen to provide the modulation and demodulation of FSK at the 444 MHz frequency that was desired.   The Melexis TH7122 transceiver was chosen for its low power consumption, FSK and FM support, ability to interface with external demodulators at the intermediate frequency and the fact that it has previously flown in space. The transceiver will be transmitting and receiving data between the satellite and the ground station.   Melexis recommended that for high selectivity and improved receiver performance, an external IF receiver and demodulator should be used. To improve receiver sensitivity a separate FSK IC that demodulated FSK at 10.7 MHz was used from New Japan Radio.
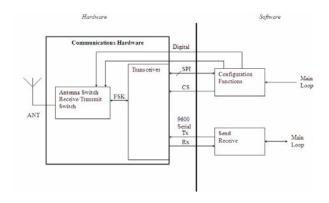

Figure 21: Hardware/Software interface of the communications system

Transmit/Receive Selection

With the half duplex system, a Transmit/Receive switch was chosen to isolate the input from the output of the amplifier. A Hittite HMC190MS8 RF switch provided the proper switching capabilities at the power and frequency of the satellite's operation. The system will have

redundancy with a dual antenna system. To provide for this dual antenna system, another Hittite RF switch and coaxial connection were added. The best antenna to operate with is then chosen during the preamble of an incoming message by looking at the RSSI values from the receiver and switching between both antennas. Both switches are controlled by the C & DH subsystem.

Antennas

The antennas transmitting the signal will be quarter-wave whips. The antenna will be 17.5 cm in length; based on a quarter of the wavelength of the system frequency. The antennas will be mounted on opposite faces of the satellite; this will provide optimal coverage for the satellite when the satellite is not over the poles of the earth. The entire aluminum chassis of the satellite and the copper on the exterior panels holding the solar panels will act as the required ground plane for the antennas. Each antenna will be connected to the communications board with low loss coax and 90 degree SMA connectors.
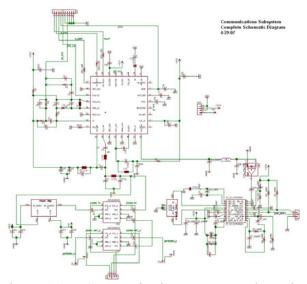

Figure 22: Communications system schematic with IC transceiver, PA, and IF IC demodulator

Power Amplifier

The RF power amplifier is needed to amplify the signal to have enough gain for the signal to successfully be received at the ground station from the satellite's low Earth orbit. A Mitsubishi RA07M4047M amplifier module was chosen to boost the 10dBm signal from the transceiver after a link analysis budget showed that the power required to successfully transmit a signal was a minimum of 0.66 W. With the Mitsubishi amplifier, the system can successfully operate at just over 1 W and still be inside the power budget constraints.
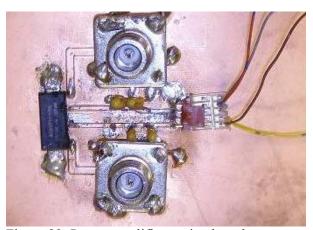

Figure 23: Power amplifier testing board

SOFTWARE

The dataflow of the system will be handled by the microcontroller. There is a main execution loop that will only be interrupted by certain events, such as thermal limits being breached or power loss. The software produced is by no means an operating system, but rather a script that handles all the interactions with the hardware. There are certain features that must be implemented on this script. All the hardware interfaces should be wrapped around driver functions and the commands and procedures are included in library functions and finally the OS-like functions conform into a separate library.
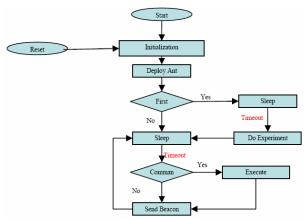
Figure 24 : Top level software design

The software must also include fail safe mechanisms. Things like redeployment of the antennas, power loss during an experiment or communication loss should be handled properly. Most of this should be accomplished by making use of the internal EEPROM of the microcontroller as a log. When important processes are being executed, appropriate flags should be set on EEPROM so that on the event of a power failure, the current executing experiment can be discarded. Upon a reset the initial processes must check EEPROM to see which tasks have been previously completed. All critical processes should include rollback mechanisms for cleaning the data lost. Another possible failure is data corruption, which data triplication should reduce and Hamming encoding should even allow data recovery for single bit errors in the packet headers.

Communications Software

The communications portion of the software runs as follows. Upon deployment of the antennas, the communications system on the satellite will periodically transmit beacon packets. The beacon packets serve to let the ground station know that the satellite is within the communications window. Once the ground station picks up a beacon packet, it can then initiate a connection with the satellite. The ground station sends a SYN packet, and the satellite responds with an ACK packet. The satellite then sends a SYN packet to the ground station, and it responds with an ACK packet to the satellite. If the satellite sits idle for too long, that is, it doesn't receive anything from the ground station, it will assume that the ground station is no longer operational, disconnect, and begin sending beacon packets again.

Once a connection is established, the ground station can issue commands to the satellite. If a ground station user assumes that the connection has been lost, a PING packet can be sent to the satellite. If no ACK packet is received, the ground station assumes that the satellite has disconnected and attempts to reconnect. The satellite can also be asked for a calibration data packet—a single data packet whose contents are already known by the ground station. This is to ensure that the data transmitted by the satellite is valid and being transmitted properly.

When asked for the data, the satellite begins sending data packets to the ground station. The packet headers are hamming encoded and the data portion of the packet has a checksum attached. The ground station receives each packet and performs a checksum algorithm on the data. If the ground station's checksum and the data packet's checksum match, the data packet is considered valid. Once all of the data packets have been sent by the satellite, it then sends a FIN packet to the ground station to inform it that all of the data has been sent. For any invalid packets or packets that weren't received by the ground station, the ground station will issue a retransmit request for each packet to the satellite. The satellite sends the requested packets as many times as the ground station asks for them. Once the ground station is satisfied that all of the data has been received, it then saves it to a file.

When the ground station has finished interacting with the satellite, a disconnect (DISCON) request packet can be sent to the satellite. As a response, the satellite will echo the DISCON packet back to the ground station. After this takes place, both the ground station and the satellite consider the connection closed.
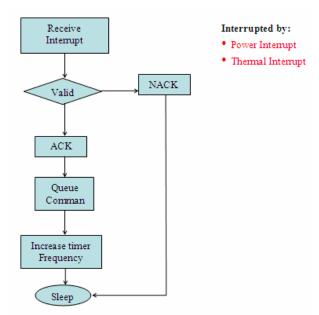
Figure 25: Communications subsystem receive interrupt chain

CONCLUSIONS

The interdisciplinary nature of this project presented a new and exciting challenge for the BillikenSat-II team. The Bio-Fuel cell payload provided a unique opportunity for our team to engineer a satellite to meet the rigorous requirements for payload operation. Bio-Fuel cells constitute a novel and innovative power alternative for space applications, and this long term outcome served as the key motivational factor for the project. BillikenSat-II has been designed to test the viability of Bio-Fuel cells in space, while at the same time restricting to the stringent specifications of the CubeSat standard. The inter-departmental work involved in this project presented the greatest challenge but was also the most significant learning opportunity. At its top-most level, any satellite design project is a systems engineering enterprise, and as such, the integration and systems interfacing challenges were the most significant to overcome.

ACKNOWLEDGEMENTS

REFERENCES

1. Redd, F.J. and G.E. Powell, "Project Thermion: Demonstration of Thermionic Heat Pipe in Microgravity," Proceedings of the 9th Symposium on Space Nuclear Power Systems, Albuquerque, NM, January 1992.

2. Folkman, S.L. and F.J. Redd, "Gravity Effects on Damping of Space Structure with Joints," Journal of Guidance, Control & Dynamics, vol. 13, No. 2, March-April 1990.

3. Wyatt, C.L., Radiometric Calibration: Theory and Methods, Academic Press, New York, 1978.

4. Galysh, I., McGuire, J., Heidt, H., Niemi, D. and Dutchover, G., CubeSat: Developing a Standard Bus for Pico-Satellites, The StenSat Group.

5. "Aluminum Material Property Data" Automation Creations Inc., Blacksburg Virginia URL: http://www.matweb.com/search/SpecificMaterial.asp?bassnum=MA6061T6 [cited 8 Oct. 2006].

6. Thomson, William T. and Dahleh, Marie Dillon., "Theory of Vibration with Applications," 5th ed., Prentice Hall, Upper Saddle River, New Jersey, 1998, p. 5-13,49-53.

7. Rao, Singiresu S., "Mechanical Vibration" 4th ed. Prentice Hall, Upper Saddle River, New Jersey, 2003.

8. Cengel, Y.A., "Radiation Heat Transfer," Introduction to Thermodynamics and Heat Transfer, 1st ed., International Ed., The McGraw-Hill Companies, Inc., New York, 1997, p. 629.

9. DeWitt, F.P., Incropera, D.P., Fundamentals of Heat and Mass Transfer, 5th ed., John Wiley & Sons, Inc., New York, 2002, p. 931.

10. Fleming, H., "DTU Satellite Systems and Design Course, Cubesat Thermal Design," Danish Space Research Institute, August 2001. URL: http://www.cubesat.auc.dk/documents/Cubesat_Thermal_Design.pdf [cited 18 Oct. 2006].

11. "Boedeker Plastics, Inc., " PEEK (PolyEtherEtherKetone) Specifications, URL: http://www.boedeker.com/peek_p.htm [cited 9 Dec. 2006].

12. US Sensors, "Thin Film Platinum RTD's." URL: http://www.ussensor.com/prod_rtds_thin_film.htm [cited 9 Dec. 2006].

13. Minco, "Kapton (Polyimide) Thermofoil™ Heater Model HK5544." URL: http://www.minco.com/heater_config/model.aspx?PN=HK5544 [cited 9 Dec. 2006].

14. K&K Associates, "Thermal Finishes 1," URL: http://www.tak2000.com/data/finish.htm [cited 5 May 2007].

15. Brewster, M. Q., "Thermal radiative transfer and properties"1 ed., Wiley, New York, 1992.

16. "DNPER-1 Launch Vehicle," Kosmotras International Space Company, URL: http://www.kosmotras.ru/rndnepr2.html [cited 17 April 2007].

17. "NORAD Two-Line Element Sets Current Data," Celestrack. URL: http://celestrak.com/NORAD/elements/ [cited 6 March 2007].

18. "ADIS 16100: ±300°/sec Yaw Rate Gyro with SPI Interface," Analog Devices, URL: http:://analog.com [cited 17 Feb. 2007].

19. Kumar, R. R., Mazanek, D. D., and Heck, M. L., "Simulation and Shuttle Hitchhiker Validation of Passive Satellite Aerostabilization," AIAA Journal of Spacecraft and Rockets, Vol. 32, No. 5, 1995 pp. 806-811.

20. Sidi, M. J., Spacecraft Dynamics and Control, Cambridge, New York, 2005, Chap. 4, 6 and 7.

21. Pais, D. and Jayaram, S., Satellite Passive Attitude Stabilization Using Permanent Magnets – Dyanmic Model and Simulation, AIAA Region V Student Conference 2007 Man # 83702.

22. Filipski, M. N., Abdullah E. J., "Nanosatellite Navigation with the WMM2005 Geomagnetic Field Model," Turkish Journal of Eng. Env. Sci., Vol. 30, 2006 pp. 43-55.

23. Wertz, J. R., Larson, W. J., Space Mission Analysis and Design, 3rd ed., Microcosm Press, Torrance CA, 1999 pp. 215.

24. Levesque. J., "Passive Magnetic Attitude Stabilization using Hysteresis Materials," Universite de Sherbrooke, SIgMA-PU-006-UdeS, Sept 2003. URL: http://www.geocities.com/jflev/cubesim.htm [cited 11 March 2007].

25. Morrish, A. H., The Physical Principles of Magnetism, IEEE Press, New York, 2001.

26. Whisnant, J. M., Anand, D. K., Psiacane, V. L., and Sturmanis, M., "Dynamic Modeling of Magnetic Hysteresis," AIAA Journal of Spacecraft and Rockets, Vol. 7, No. 6, 1970 pp. 697-701.

27. Fischell R. E., "Magnetic Damping of the Angular Motions of Earth Satellites," ARS Journal, Vol. 31, No. 9, 1961 pp. 1210.